2024 14th International Symposium on Communication Systems, Networks and Digital Signal Processing (CSNDSP) | 979-8-3503-4874-3/24/$31.00 ©2024 IEEE | DOI: 10.1109/CSNDSP60683.2024.10636494

Converged Satellite to Fiber QKD links: A feasibility analysis

Aristeidis Stathis
School of Electrical and Computer Engineering
National Technical University of Athens
Athens, Greece
stathisaris@mail.ntua.gr

Argiris Ntanos
School of Electrical and Computer Engineering
National Technical University of Athens
Athens, Greece
ntanosargiris@mail.ntua.gr

Nikolaos K. Lyras
School of Electrical and Computer Engineering
National Technical University of Athens
Athens, Greece
lyrasnikos@mail.ntua.gr

Giannis Giannoulis
School of Electrical and Computer Engineering
National Technical University of Athens
Athens, Greece
jgiannou@mail.ntua.gr

Athanasios D. Panagopoulos
School of Electrical and Computer Engineering
National Technical University of Athens
Athens, Greece
thpanag@ece.ntua.gr

Hercules Avramopoulos
School of Electrical and Computer Engineering
National Technical University of Athens
Athens, Greece
hav@mail.ntua.gr

***Abstract*— This paper presents a comprehensive feasibility analysis designed to model Low Earth Orbit (LEO) satellite-to-ground communications for Quantum Key Distribution (QKD), focusing on the 1550nm wavelength to facilitate the distribution of information through fiber segments. Discrete Variable Decoy State Polarization-based BB84 protocol is assumed whereas various detection setups and environmental conditions are simulated. Our analysis focuses on the receiver's design in terms of aperture and focal length to deliver a general framework by examining the coupling efficiency, a parameter strongly affecting the QKD satellite downlink. Through detailed simulation, we identify optimal configurations and operational parameters for various receiver designs, significantly enhancing the efficiency and reliability of satellite-to-ground QKD systems. The findings offer promising directions for extending the range of QKD systems, potentially revolutionizing secure communications by integrating satellite-transmitted quantum keys with terrestrial fiber networks. This study not only underscores the feasibility of advancing satellite-to-ground QKD technology but also lays the groundwork for future innovations in global quantum communications infrastructure.**

Keywords—QKD, satellite-to-ground communication, SMF coupling

I. Introduction

Quantum Key Distribution (QKD) represents a paradigm shift in secure communications, leveraging the principles of quantum mechanics to enable two parties to produce a shared random secret key known only to them, which can then be used to encrypt and decrypt messages. The advent of satellite-to-ground QKD [1] has further broadened the horizons of secure communication, enabling global reach beyond the limitations of terrestrial fiber networks [2], offering a new pathway to achieving global secure communication coverage. Yet, the integration of satellite QKD systems with existing fiber networks and the extension of their capabilities to serve wider, more geographically dispersed areas remain less explored, particularly in the context of rural and remote regions. This work positions itself within this evolving narrative by specifically addressing the gap between the high potential of satellite-based QKD systems for global coverage and the practical challenges of extending their reach through effective integration with ground-based fiber networks. More specifically, this paper presents a feasibility analysis between Low Earth Orbit (LEO) satellites and various Optical Ground Stations (OGSs) located in rural areas. The simulation focuses on the 1550 nm wavelength, chosen for its potential to distribute qubits further through fiber segments post initial ground reception, addressing a critical challenge in extending the range of QKD systems. Technical challenges such as the effect of turbulence in coupling efficiency from the receiving telescope to a Single Mode Fiber (SMF) are discussed. Variables such as atmospheric turbulence, receiver aperture size and focal length are modelled to understand their effects on telescope to fiber coupling efficiency. The choice of the 1550 nm wavelength for communication further reflects a targeted approach to enhance the compatibility between satellite signals and terrestrial fiber segments, aiming to mitigate the loss and extend the effective range of QKD systems beyond their current limitations. By conducting a detailed feasibility analysis and exploring the technical intricacies of coupling efficiency, atmospheric conditions, along with the integration with fiber segments, this study contributes to the practical realization of a global, secure quantum communication network, paving the way for the next generation of secure communications.

The remainder of the paper is organized as follows. Section II provides the overall system model and assumptions. Section III gives the modelling of the LEO-to-ground QKD link, as well as a brief description for the QKD protocol. Finally, section IV the feasibility results are presented and discussed while section V concludes this work.

II. System Model

In this section, the system model and its assumptions are presented. Our study focuses on employing telescopes with diverse design parameters (such as aperture diameter, obscuration ratio, focal length, etc.) as receivers. LEO satellites are selected as the preferred transmitters, attributed to their efficacy in ensuring a sufficient link budget for effective key distillation [3]. It's important to note that our analysis is limited to the downlink scenario to avoid the challenges associated with the lossy and turbulent uplink

Authorized licensed use limited to: UNIVERSIDADE DE SAO PAULO. Downloaded on July 11,2026 at 04:50:11 UTC from IEEE Xplore. Restrictions apply.

transmission. The study specifically addresses the case where the quantum signal is within the C-band, i.e., 1550nm. The wavelength selection is based, not only as an atmospheric transmission window for satellite downlinks but also due to its compatibility with existing optical devices as well as for the compatibility with the standard optical fibers, thereby facilitating a unified approach to both fiber and free space transmission. In terms of the detection setup, Superconducting Nanowire Single-Photon Detectors (SNSPDs) are considered for the detection. SNSPDs are recognized for their exceptional performance over a broad wavelength spectrum pertinent to satellite-based quantum communications. In this study, we also assume fiber coupling, which enables signal transmission over extended distances through low-loss optical fibers to a secure location for detection which may be in a different building with respect to the receiving telescope or in a different security perimeter. This approach, often referred to as intermodal QKD, has been recently proposed in the literature [4] and is particularly beneficial because it enables multiple users to utilize the same optical telescope, or establish a trusted zone near the telescope. Figure.1 provides a schematic overview of the envisioned architecture, where OGSs can be located outside from the terrestrial grid where the altitude is usually lower and the artificial background noise may affect the QKD performance [5]. Considering the above, photons can be transferred from the OGS to the urban environment via telescope-to-fiber coupling without the need for an intermediate trusted node.

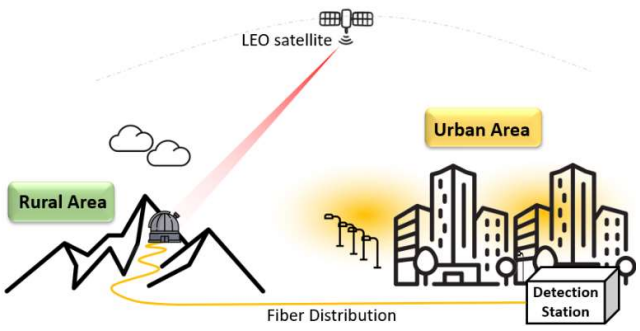


Fig. 1. Architecture of converged satellite/fiber QKD communication, enabled via telescope-to-fiber coupling.

III. LEO-TO-GROUND QKD LINK MODELLING

Among the phenomena that impair the optical/quantum satellite link, cloud occurrence is the dominant one which causes the blockage of the link [6], [7]. However, even under cloud free line of sight conditions propagation through atmosphere still degrades the performance of the optical communication system. For the study presented in this work, our LEO-to-ground link modelling focuses on the geometrical losses, losses due to atmospheric transmission and turbulence as well as the coupling from the telescope to the SMF. All the above are considered employing the polarization-based DS-BB84 protocol. Our approach accounts for the challenges posed by photon transmission efficiency, signal attenuation due to atmospheric effects under Cloud Free Line of Sight (CFLOS) conditions and system design. This targeted modelling enables us to isolate key factors affecting the satellite-to-ground QKD performance under CFLOS conditions providing insights into optimizing the QKD communication for practical deployments.

A. Geometrical Loss

Geometrical loss in satellite-based communications is a critical factor that impacts the efficiency and reliability of signals transmitted between satellites and ground stations or between satellites. This type of loss is inherent to the propagation of electromagnetic waves over long distances through the vacuum of space or the atmosphere, without considering the effects of atmospheric absorption, scattering, or other forms of signal degradation. For a LEO satellite in orbit, the distance between the satellite and the ground is determined by the satellite's elevation angle and can be calculated using Eq. (1):

$$d(\theta) = R_e\left(\sqrt{\left(\frac{H+R_e}{R_e}\right)^2 - cos^2\,\theta} - sin\,\theta\right) \quad (1)$$

, where H is the satellite's altitude above the Earth's surface, R_e is the Earth's radius, and θ is the elevation angle. The geometrical loss factor can then be calculated using (2) according to [8]:

$$A_{geo} = \left(\frac{\lambda}{4\pi\, d(\theta)}\right)^2 \times \left(\frac{\pi\, D_r}{\lambda}\right)^2 \times \left(\frac{8}{\theta_B^2}\right) \quad (2)$$

with θ_B being the half-width divergence angle of the transmitted beam assuming Gaussian beam profile.

B. Atmospheric Transmission and Turbulence

The clear sky atmospheric transmittance also varies with the elevation angle of the satellite. The atmospheric transmittance can be calculated using the following expression [9]:

$$L_a = L_{zen}^{\left(\frac{1}{\cos(\zeta)}\right)} \quad (3)$$

where L_{zen} is the transmittance for a vertical link at a specific wavelength and ζ (in radians) is the zenith angle of the link. Here L_{zen} is provided for clear sky conditions.

Another important factor affecting the performance of a QKD-downlink between a LEO-satellite and an OGS, is the rapid variations in the intensity and phase of light, called scintillation. Scintillation can significantly affect FSO communication links, leading to signal intensity fluctuations at the receiver [8]. These fluctuations occur due to thermal variations that alter the refractive indices within small air pockets, causing the light beam to diffract and wander [8]. In satellite downlinks, the beam front's size generally exceeds that of these air pockets, mitigating the impact of scintillation on the receiver. Nonetheless, considering scintillation's effects remains crucial. Scintillation intensity is typically classified as weak, moderate, or strong, depending on the

Authorized licensed use limited to: UNIVERSIDADE DE SAO PAULO. Downloaded on July 11,2026 at 04:50:11 UTC from IEEE Xplore. Restrictions apply.

refractive index structure parameter $C_n^2\ (m^{-2/3})$. This parameter's value is primarily influenced by atmospheric conditions, including temperature and pressure. This study uses the modified expression of the Hufnagel-Valley model which considers the altitude of the ground station and the elevation angle of the link. The calculation of the $C_n^2\ (m^{-2/3})$ value can be found in [10]:

$$C_n^2(h) = A_0\, exp\left(-\frac{H_{GS}}{700}\right) exp\left(\frac{H_{GS}-h}{100}\right) 5.94 \times \\ \times 10^{-53}(\frac{u_{rms}}{27})^2 h^{10}\, exp\left(-\frac{h}{1000}\right) \\ + 2.7 \times 10^{-16} exp\,(-\frac{h}{1500}) \quad (4)$$

The calculation of the refractive index structure parameter, $A_0\ (m^{-2/3})$ involves the average wind speed, u_{rms} (m/s), along the slant path using the Bufton model and the altitude of the ground station, $H_{GS}\ (m)$, and the height above the ground station, h (m). The scintillation index for weak, average, and strong turbulence, for a plane wave approximation under the assumption of the Kolmogorov model, can be determined using the following expression [8], [11]:

$$\sigma_{I,pt}^2 = \exp\left(\frac{0.49\sigma_R^2}{\left(1+1.11\sigma_R^{\frac{12}{5}}\right)^{\frac{7}{6}}}\frac{0.51\sigma_R^2}{\left(1+0.69\sigma_R^{\frac{12}{5}}\right)^{\frac{5}{6}}}\right) - 1 \quad (5)$$

where σ_R is the Rytov index which when considering the OGS's height, can be calculated as [8], [11]:

$$\sigma_R^2 = 2.25k^{\frac{7}{6}}sec^{\frac{11}{6}}(\zeta)\int_{H_{GS}}^{H_{Turb}} C_n^2(h)(h-H_{GS})^{\frac{5}{6}}dh \quad (6)$$

Where k is the wavenumber and H_{turb} denotes the maximum turbulence altitude which is considered negligible for altitudes higher than 20 km. Finally, the scintillation loss (dB) induced by turbulence for a given outage probability p_0 is calculated according to the Kolmogorov model by including the aperture averaging effect as follows [12]:

$$L_{sci} = 4.343 \times \left[erf^{-1}(2p_0-1)\cdot[2\ln(\sigma^2{}_I+1)]^{\frac{1}{2}} \right. \\ \left. -\frac{1}{2}\ln(\sigma^2{}_I+1)\right] \quad (7)$$

C. Coupling

Addressing the technical challenge of coupling an optical satellite signal into a ground receiver involves overcoming unique obstacles compared to traditional radio frequency (RF) communications. Optical satellite communications encounter several challenges due to the nature of light propagation and atmospheric conditions. Coupling from free space to Single-Mode Fiber (SMF), particularly for large telescopes, presents significant challenges in the presence of turbulence, as it requires matching between the incoming beam's intensity distribution and phase front [13]. To address this issue, Adaptive Optics (AO) systems are utilized [14], leading to a notable improvement in fiber coupling efficiency. These systems enable to achieve coupling efficiencies over 50%, even in the case of large telescopes [13]. Atmospheric turbulence can strongly deteriorate coupling efficiency. The degree to which turbulence impacts the coupling efficiency depends on the Fried parameter r_0, which is defined by the following expression [8]:

$$r_0 = \left[0.42\ k^2 sec(\zeta)\int_{H_{GS}}^{H_{Turb}} C_n^2(h)dh\right]^{-3/5} \quad (8)$$

In turn the coupling efficiency due to the effect of turbulence is calculated as follows [8], [15] :

$$\eta_{FC} = \left[1+\gamma\left(\frac{D_r}{r_0}\right)^{5/3}\right]^{-\frac{6}{5}} \quad (9)$$

, where factor γ account the level for AO or tip tilt correction in the receiver subsystem and is set to 1, 0.28, and 0 for no correction, tip tilt correction and full AO correction, and r_0 denotes the Fried's parameter integrated along the slant path for up to a maximum altitude of H_{turb} [8]. To account for the efficiency of the receiving telescope, as well as for its secondary mirror and its focal length, the optical coupling efficiency is included as in [16]:

$$\eta_0 = 2\left[\frac{\exp(-\beta^2)-\exp(-\beta^2\,a^2)}{\beta\sqrt{1-\alpha^2}}\right]^2 \quad (10)$$

, where α, β are given by [16]:

$$a = \frac{D_{obs}}{D_r},$$

$$\beta = \pi\frac{D_r}{4\lambda}\frac{MFD}{f} \quad (11)$$

Finally, the overall telescope to SMF coupling efficiency is defined as:

$$\eta_c = \eta_0 \cdot \eta_{FC} \quad (12)$$

D. DS-BB84 Protocol

The Decoy-State BB84 (DS-BB84) was utilized as a P&M protocol employing the "weak + vacuum" configuration, as described in [17]. To counter the Photon Number Splitting (PNS) attack, decoy and vacuum states are incorporated into the traditional BB84 protocol, enabling the precise measurement of both background noise and the channels loss, rendering the protocol able to detect eavesdropping attacks. As a result, the decoy state protocol provides reduced vulnerability to PNS attacks enabling higher mean photon numbers per pulse, thus increasing the maximum distance reach as well as the Secure Key Rate (SKR). The normalized SKR (bps/pulse) is lower bounded by the following inequation [17]:

$$\frac{SKR}{f_{rep}} \geq\ q\{Q_1[1-H_2(e_1)] - Q_\mu f(E_\mu)H_2(E_\mu)\}\eta_{dead} \quad (13)$$

Authorized licensed use limited to: UNIVERSIDADE DE SAO PAULO. Downloaded on July 11,2026 at 04:50:11 UTC from IEEE Xplore. Restrictions apply.

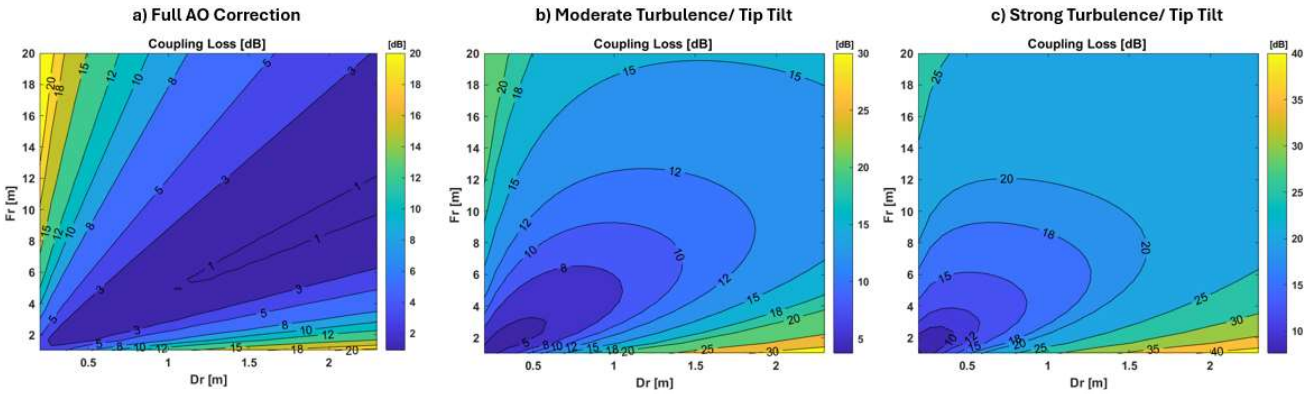


Fig. 2. Contour plots of SMF coupling loss (dB) over focal length Fr and receiver aperture diameter Dr for a) Full AO correction, b) Tip-Tilt correction for $C_n^2=10^{-14}$ $m^{-2/3}$ and c) Tip-Tilt correction for $C_n^2=10^{-13}$ $m^{-2/3}$ for an elevation angle of 90°

where q is the protocol efficiency, the subscript μ is the average photon number per signal in signal states, Q_μ and E_μ are the gain and the Quantum Bit Error Rate (QBER) of signal states, respectively, Q_1 and e_1 are the gain and the error rate of the single photon state in signal states, respectively, $f(x)$ is the bi-directional error correction rate, $H_2(x)$ is the binary entropy function and η_{dead} is the dead time efficiency of the detector calculated according to [18].

IV. Feasibility Analysis Results and Discussion

Micius satellite is the only satellite to date that has demonstrated successful satellite-to-ground QKD communication. Given the groundbreaking achievements of the Micius mission, it often serves as a reference in the literature for advancing the research in the field of quantum communication [19]. Therefore, in our study, we also adopt some of the specifications and operational parameters used in the Micius mission as a baseline for our simulations with the exception of the wavelength of the quantum signal which is assigned to 1550 nm.

Table 1 Simulation input parameters

Symbol	Parameter	Value
λ	quantum channel wavelength	1550 nm
f	Emission rate	100 MHz
H_{sat}	Satellite orbit altitude	550 km
D_{Tx}	Tx telescope aperture diameter	0.3 m
ε	Min. elevation angle	20°
σ_p	Pointing error variance [20]	0.7 μrad
η_{Bob}	Detector's setup loss	1.5 dB
L_a	Vertical atmospheric transmittance [21]	0.78
H_{rad}	Nighttime Background solar radiance [22]	$1.5 \times 10^{-5} m^2 sr\ \mu m$
H_{turb}	Maximum Altitude for slant path integration	20 km
p_0	Outage Probability	1%
Ω_{FOV}	Receiver's FOV	100 μrad
λ_{pass}	Filter's spectral passband	0.1 nm
η_{filter}	Filters efficiency	0.7
μ, ν	Mean signal, decoy photon/pulse	0.7, 0.1
η_{SNSPD}	SNSPDs detection efficiency	0.85
DCR_{SNSPD}	SNSPDs dark count rate	5 cps
t_{gate}	Effective gate time window	1 ns
τ_{dead_SNSPD}	Dead time SNSPD	30 ns
e	Error probability for noise counts	50%

The parameters that are considered in our simulations are listed in Table 1 and are typical. For this study the simulated LEO passage is considered to be optimum, that is a single pass of the satellite is able to reach elevation angle of 90°. Additionally satellite-to-ground communication is only assumed to be possible for elevation angles greater than 20°. Fig. 2 presents a contour plot illustrating the SMF coupling efficiency η_c, calculated based on eq. (12), as a function of receiver's telescope Fr (m) and aperture diameter Dr (m) considering full AO and tip-tilt correction amid moderate ($C_n^2=10^{-14}$ $m^{-2/3}$) and strong turbulence ($C_n^2=10^{-13}$ $m^{-2/3}$). For this calculation a satellite elevation angle of 90^o is assumed.

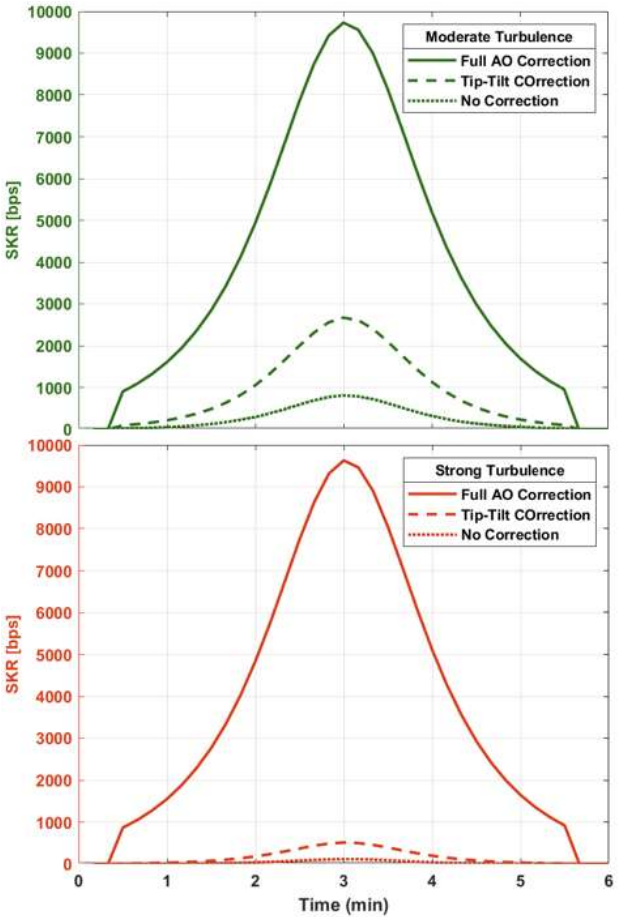


Fig. 3 Calculated SKR over a single satellite pass considering, a) moderate and b) strong turbulence $C_n^2=10^{-14}$, AO, tip-tilt and no correction, γ=0, 0.28 and 1.

Authorized licensed use limited to: UNIVERSIDADE DE SAO PAULO. Downloaded on July 11,2026 at 04:50:11 UTC from IEEE Xplore. Restrictions apply.

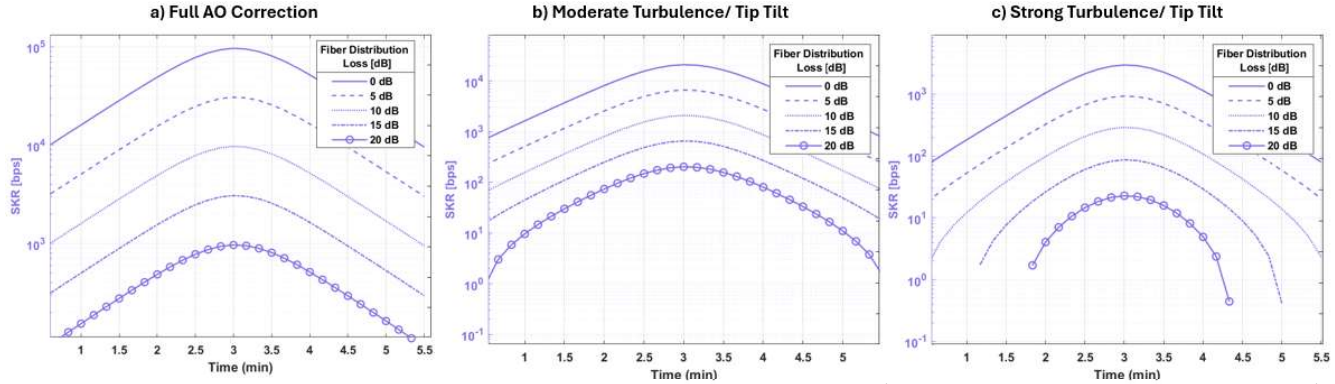


Fig. 4 SKR over time for a) Full AO correction, b) Tip-Tilt correction for $C_n^2=10^{-14}$ $m^{-2/3}$ and c) Tip-Tilt correction for $C_n^2=10^{-13}$ $m^{-2/3}$ for different fiber distribution loss values (dB).

The receiver is located at an altitude of 500 m. Given the direct influence of atmospheric turbulence, eq. (9) is utilized to incorporate this effect. Specifically, for the AO correction we set the value γ in eq. (9) to be equal to 0 whereas for the case of tip-tilt correction this value is set to be 0.28 and 1 for no correction at all. The efficiency of the telescope is accounted through eq. (10) where D_{obs} is kept constant at 0.1 m. It should be noted here that secondary mirrors of reflector telescopes are often placed within the path of the beam so that it blocks part of the primary mirror and affects the diffraction spreading, although the loss is <1 dB for a secondary mirror diameter up to 25% of the ratio of the primary mirror diameter (Dr) [23]. From Fig. 2.a. is evident that full AO correction negates the impact of turbulence on coupling efficiency. It should be noted here that this is an ideal approximation accounting for a lossless AO system. This scenario assumes that the effect of turbulence in SMF coupling is completely neglected, therefore only the coupling loss due to the geometry (η_0) of the telescope's optics (obscuration, receiver aperture, focal length, etc.) determine the coupling efficiency. By choosing an optimal focal length it is calculated that a coupling efficiency of up to of 81% (~1dB) can be achieved, as also described in [16]. On the other hand, when tip-tilt correction is applied (Fig. 2b) the coupling efficiency is greatly affected by the turbulence with the optimum coupling efficiency achieved when the receiver's focal length and diameter exhibit a seemingly linear correlation. Additionally, it is also observed that for larger telescopes SMF coupling seems much more challenging and yields high loss compared to smaller ones for both moderate and strong turbulence cases. Finally, for the assumed OGSs receiver setup ($D_r = 1m, fr = 10m$) the overall coupling loss is calculated to be about 11dB and 19dB for moderate and strong turbulence respectively.

Fig. 3a, 3b, illustrate the calculated SKR during a single satellite pass at 1550 nm over an OGS with a 1 m receiver diameter located in rural environment at 500 m altitude during nighttime considering moderate and strong turbulence, respectively. The use of SNSPDs is assumed in the receiving terminal with their characteristics shown in Table 1 above. For the case of moderate turbulence depicted in Fig, 3b, it is observed that SKRs of up to 95 kbps can be achieved for the case of full AO correction. This high value so attributed to the relatively low link loss which reaches a minimum less than 30dB for elevations of *90°*. When tip-tilt correction is applied, the calculated SKR is dropping down to almost 12 kbps per passage due to the decreased link loss whereas in the case of no correction the increased coupling loss induced by turbulence makes the key distillation impractical for low elevation angles, thus limiting the QKD communication time window. Conversely, amid strong turbulence the SKR remains unaffected when full AO correction is applied. For the case of tip tilt, turbulence strongly affects the QKD performance, limiting the maximum achievable generated SKR to more than an order of magnitude, compared to the ideal full AO correction scenario.

Finally, for the case of no correction maximum key rates of about 400 bps are being calculated, yet the communication time window is limited to about 2 minutes.

It should be noted again, the provided results assume an ideal satellite pass, where the elevation angle reaches 90 degrees of elevation. In a more realistic scenario, satellites are often seen with much lower maximum elevation angles per pass. Considering the above, and by accounting the increased coupling loss due to turbulence, it is suggested that the case of no correction is impractical for satellite-to-ground QKD links.

Fig. 4 provides the expected SKR values over time assuming an ideal AO system, and a tip-tilt correction system under moderate and strong turbulence. For the case of full AO correction (Fig. 4a), an additional fiber distribution link budget of 20dB is possible, allowing up to 100 km fiber extension, (assuming the ideal case of dark fiber with attenuation of 0.2dB/km), yielding almost up to 1 kbps SKR. In a more realistic scenario, 20dB usually allows for shorter distances due to additional losses introduced from multiple connection points and bending losses. Nonetheless, for this scenario, high key rates can be transferred from the telescope site to remote location without the need for a trusted node configuration. To continue, in the case where only tip-tilt correction is applied (Fig. 4b), the same distance can be achieved, but with limited key rates and reduced distillation window. Comparing between the ideal case of full AO correction and tip-tilt correction under moderate turbulence, the overall generated key volumes for the case of 20dB additional loss due to further fiber distribution are calculated to be 136 kbits and 22.4 kbits over the five (5) minute time window, respectively. Finally, in Fig. 4c the effect of the strong turbulence on the key rates is presented, assuming once again tip-tilt correction. As seen previously, the effect of turbulence is much stronger for lower elevation angles,

Authorized licensed use limited to: UNIVERSIDADE DE SAO PAULO. Downloaded on July 11,2026 at 04:50:11 UTC from IEEE Xplore. Restrictions apply.

resulting in a much more limited communication time window. Assuming an additional 10dB loss for the fiber distribution segment, key rates of up to 250 bps are possible. It should be noted that this value can only be achieved assuming that the satellite reaches a high enough elevation angle. Comparing to the case of moderate turbulence, the maximum SKRs achieved with an additional 10dB loss, are calculated to be about 10 times lower, whereas the total volume of distilled keys about 8 times lower (246 kbits and 30 kbits respectively), due to the additional limit in the communication time window.

V. Conclusions

To conclude, this feasibility analysis delves into the intricate dynamics of LEO satellite-to-ground QKD communication. By simulating various receiver designs, atmospheric conditions, and turbulence effects, we identify key parameters influencing the performance of satellite-to-ground QKD links. Our findings highlight the critical role of adaptive optics in mitigating turbulence-induced losses and improving fiber coupling efficiency. Moreover, the potential of integrating satellite-transmitted quantum keys with terrestrial fiber networks is demonstrated, paving the way for a global, secure quantum communication infrastructure. Despite challenges posed by atmospheric turbulence, our analysis underscores the feasibility and promise of advancing satellite-to-ground QKD technology.

Acknowledgements

This work was supported in part by the European Commission through the project LaiQa, under grant agreement No. 1011335245.

References

[1] C.-Y. Lu, Y. Cao, C.-Z. Peng, and J.-W. Pan, "Micius quantum experiments in space," *Rev. Mod. Phys.*, vol. 94, no. 3, p. 035001, Jul. 2022, doi: 10.1103/RevModPhys.94.035001.

[2] R. Bedington, J. M. Arrazola, and A. Ling, "Progress in satellite quantum key distribution," *Npj Quantum Inf.*, vol. 3, no. 1, Art. no. 1, Aug. 2017, doi: 10.1038/s41534-017-0031-5.

[3] A. Ntanos *et al.*, "MEO satellite-to-ground Decoy-State QKD links realistic performance analysis," in *International Conference on Space Optics—ICSO 2022*, SPIE, 2023, pp. 1116–1130. Accessed: Mar. 07, 2024. [Online]. Available: https://www.spiedigitallibrary.org/conference-proceedings-of-spie/12777/127772N/MEO-satellite-to-ground-Decoy-State-QKD-links-realistic-performance/10.1117/12.2690001.short

[4] F. Picciariello *et al.*, "Intermodal quantum key distribution field trial with active switching between fiber and free-space channels." arXiv, Oct. 26, 2023. Accessed: Jan. 30, 2024. [Online]. Available: http://arxiv.org/abs/2310.17441

[5] A. Tomaello, C. Bonato, V. Da Deppo, G. Naletto, and P. Villoresi, "Link budget and background noise for satellite quantum key distribution," *Adv. Space Res.*, vol. 47, no. 5, pp. 802–810, Mar. 2011, doi: 10.1016/j.asr.2010.11.009.

[6] "Cloud Attenuation Statistics Prediction From Ka-Band to Optical Frequencies: Integrated Liquid Water Content Field Synthesizer | Semantic Scholar." Accessed: Mar. 08, 2024. [Online]. Available: https://www.semanticscholar.org/paper/Cloud-Attenuation-Statistics-Prediction-From-to-Lyras-Kourogiorgas/1e02e4e8de8f26f88e97c44372beb564ec2b7353

[7] N. K. Lyras, C. N. Efrem, C. I. Kourogiorgas, and A. D. Panagopoulos, "Optimum Monthly Based Selection of Ground Stations for Optical Satellite Networks," *IEEE Commun. Lett.*, vol. 22, no. 6, pp. 1192–1195, Jun. 2018, doi: 10.1109/LCOMM.2018.2819174.

[8] L. C. Andrews and R. L. Phillips, "Laser Beam Propagation Through Random Media: Second Edition," *Laser Beam Propag. Random Media Second Ed.*, Sep. 2005, doi: 10.1117/3.626196.

[9] K. Kiasaleh, "On the probability density function of signal intensity in free-space optical communications systems impaired by pointing jitter and turbulence," *Opt. Eng.*, vol. 33, pp. 3748–3757, Nov. 1994, doi: 10.1117/12.181939.

[10] H. H. Hemmati Hamid, Ed., *Near-Earth Laser Communications*. Boca Raton: CRC Press, 2018. doi: 10.1201/9781420015447.

[11] H. Kaushal and G. Kaddoum, "Optical Communication in Space: Challenges and Mitigation Techniques," *IEEE Commun. Surv. Tutor.*, vol. 19, no. 1, pp. 57–96, 2017, doi: 10.1109/COMST.2016.2603518.

[12] "[PDF] Scintillation loss in optical low earth orbit data downlinks with avalanche photodiode receivers | Semantic Scholar." Accessed: Jun. 15, 2023. [Online]. Available: https://www.semanticscholar.org/paper/Scintillation-loss-in-optical-low-earth-orbit-data-Giggenbach-Moll/cce5ee506fbe1b5a7a06cadbdebf9849680ab545

[13] N. Jovanovic *et al.*, "Efficient injection from large telescopes into single-mode fibres: Enabling the era of ultra-precision astronomy," *Astron. Astrophys.*, vol. 604, p. A122, Aug. 2017, doi: 10.1051/0004-6361/201630351.

[14] R. K. Tyson and B. W. Frazier, *Principles of Adaptive Optics*, 5th ed. Boca Raton: CRC Press, 2022. doi: 10.1201/9781003140191.

[15] A. Krzic, D. Heinig, M. Goy, and F. Steinlechner, "Dual-downlink quantum key distribution with entangled photons: Prospects for daylight operation," in *Dual-downlink quantum key distribution with entangled photons: Prospects for daylight operation*, International Conference on Space Optics Dubrovnik Croatia, Oct. 2022.

[16] A. Scriminich *et al.*, "Optimal design and performance evaluation of free-space quantum key distribution systems," *Quantum Sci. Technol.*, vol. 7, no. 4, Art. no. 4, Jun. 2022, doi: 10.1088/2058-9565/ac8760.

[17] H.-K. Lo, X. Ma, and K. Chen, "Decoy State Quantum Key Distribution," *Phys. Rev. Lett.*, vol. 94, no. 23, Art. no. 23, Jun. 2005, doi: 10.1103/PhysRevLett.94.230504.

[18] P. Eraerds, N. Walenta, M. Legré, N. Gisin, and H. Zbinden, "Quantum key distribution and 1 Gbps data encryption over a single fibre," *New J. Phys.*, vol. 12, no. 6, p. 063027, Mar. 2010, doi: 10.1088/1367-2630/12/6/063027.

[19] S.-K. Liao *et al.*, "Satellite-to-ground quantum key distribution," *Nature*, vol. 549, no. 7670, Art. no. 7670, Sep. 2017, doi: 10.1038/nature23655.

[20] "Design and in-orbit test of a high accuracy pointing method in satellite-to-ground quantum communication." Accessed: Jan. 23, 2024. [Online]. Available: https://opg.optica.org/oe/fulltext.cfm?uri=oe-28-6-8291&id=428813

[21] "MODTRAN®." Accessed: Jul. 11, 2023. [Online]. Available: http://modtran.spectral.com/modtran_home

[22] C. Bonato, A. Tomaello, V. Da Deppo, G. Naletto, and P. Villoresi, "Feasibility of satellite quantum key distribution," *New J. Phys.*, vol. 11, no. 4, Art. no. 4, Apr. 2009, doi: 10.1088/1367-2630/11/4/045017.

[23] J.-P. Bourgoin *et al.*, "A comprehensive design and performance analysis of low Earth orbit satellite quantum communication," *New J. Phys.*, vol. 15, no. 2, p. 023006, Oct. 2013, doi: 10.1088/1367-2630/15/2/023006.

Authorized licensed use limited to: UNIVERSIDADE DE SAO PAULO. Downloaded on July 11,2026 at 04:50:11 UTC from IEEE Xplore. Restrictions apply.